北海道大学工学部研究報告
第102号（昭和56年）

Bulletin of the Faculty of Engineering,
Hokkaido University, No. 102 (1981)

Composition and Structure of Anodic Oxide Films on Copper in Neutral and Weakly Alkaline Borate Solutions

Masahiro SEO*, Tomoo IWATA and Norio SATO***

(Received August 30, 1980)

Abstract

Copper surfaces anodically oxidized at constant potential for 1h in deaerated neutral and weakly alkaline borate solutions were examined by using electrochemical techniques combined with Auger electron spectroscopy (AES) and X ray-photo electron spectroscopy (XPS). The thickness (1～4 nm) of anodic oxide films coulometrically estimated decreased with increasing anodic potential in the active region but increased in the passive region, irrespective of the solution pH. The anodic oxide films formed on copper in the passive region consisted of Cu_2O as an inner layer and of partly hydrated cupric oxide, $CuO_x(OH)_{2-2x}$ as an outer layer. Dehydration of the outer layer progressed with the increasing anodic potential. The active potential region of copper was divided into two parts ; Cu_2O film was directly formed on copper without any dissolution of cuprous ions in active region 1 whereas in active region 2 the formation of Cu_2O and the dissolution of cupric ions proceeded simultaneously.

Discussion was made on the formation mechanism of the outer layer in the passive region and on the dissolution mechanism of Cu_2O in the active region.

1. Introduction

Corrosion and passivity of copper in neutral and weakly alkaline solutions have not been thoroughly investigated in comparison with that in strongly alkaline solutions.[1-7] Particularly, there have been only a few studies[8] on the composition and structure of anodic oxide films on copper.

In the present paper, the composition and structure of anodic oxide films formed on copper in neutral and weakly alkaline solutions have been investigated by using electrochemical techniques coupled with Auger electron spectroscopy (AES) and X ray-photo electron spectroscopy (XPS).

2. Experimental

2. 1. Specimen preparation and anodic oxidation

Copper specimens (0.1×1.0×1.0 cm) were cut from a deoxidized copper plate (99.9%

* Department of Engineering Science.

** Central Research Institute, Fuji Denki Seizō Company, Yokosuka, 240-01, JAPAN.

purity). After annealing at 1233 K for 1 h in vacuo, the specimens were mechanically polished with emery paper, further with α-Al_2O_3 abrasives (0.3 μm) and finally electropolished in 7.3 mol · dm^{-3} ortho-phosphoric acid solution. The electrolytes used for anodic oxidation were deaerated borate solutions of pH 6.48, 8.42 and 11.50 in which the boron content was kept at 0.5 mol·dm^{-3}. The specimens were cathodically reduced at a constant current density of 0.1 A·m^{-2} for 5 min in pH 8.42 borate solution and then anodically oxidized at a constant potential for 1 h in the renewed test solution. The cupric ions dissolved into the solution during anodic oxidation were detected by the cuprizone colorimetric method. Attempts to detect dissolved cuprous ions by the cuproine colorimetric method were unsuccessful in this experiment. In order to estimate culometrically the film thickness, the cathodic reduction of anodic oxide films was performed at a constant cathodic current density of 0.1 A · m^{-2} in pH 8.42 borate solution.

2. 2. AES and XPS measurements

After anodic oxidation, the specimens were washed with doubly distilled water, dried with a jet of nitrogen gas and stored in a glass tube filled with liquid nitrogen to prevent further-oxidation from exposure in air. Auger apparatus (PHI, 540 A) was used for the measurement of composition profiles in depth. Auger spectra were taken by using a primary electron beam of 2 kV with a diameter of about 50 μm and a modulation voltage of 4 V at a frequency of 30 kHz. Depth-profiling was performed with a argon ion beam of 0.5 kV having an ion current density of approximately 5×10^{-2} A · m^{-2} at an argon pressure of 6.7×10^{-3} Pa. Further, XPS apparatus (VG, ESCA-3) was used for state-analysis of copper and oxygen in the anodic oxide films. XPS spectra of Cu $2P^{3/2}$, $2P^{1/2}$ and O 1s were taken in a vacuum of 5×10^{-8} Pa by using an X ray source of Mg K_α (1253.6 eV).

3. Results and Discussion

3. 1. Anodic oxidation of copper

Fig. 1 shows the steady state-polarization curves of copper after anodic oxidation for 1 h in pH 6.48, 8.42 and 11.50 borate solutions. The electrode potential, E_{HESS}, in the abscissa of Fig. 1 is referred to the hydrogen electrode in the same solution (HESS). The polarization curves consist of three potential regions ; active, passive and oxygen evolution. The active potential region can be further divided into two parts (active 1 and 2), since cupric ions dissolved into solution were detected in all potential regions except active region 1. In Fig. 2, the electric charge passed during anodic oxidation, Q_a, is plotted as a function of anodic potential, E_{HESS}. The curve of Q_a vs. E_{HESS} is quite similar to the polarization curve in the respective solution.

3. 2. Cathodic reduction of anodic oxide film

Fig. 3 shows the typical cathodic reduction curves of the specimens anodically oxidized in three different potential regions in pH 8.42 borate solution. The cathodic reduction curves similar to the curves shown in Fig. 3 were also obtained for the specimens anodically oxidized in the other pH solutions. Cathodic reduction, however, was always performed in renewed pH 8.42 borate solution. The potential arrest during cathodic reduction is observed at the potentials of Φ_c^1, Φ_c^2, Φ_c^3 and $\Phi_c^{3'}$, depending on the potential region of anodic oxidation. The arrest potentials of Φ_c^2 and Φ_c^3 are less noble by 150~200 mV than the corresponding equilibrium

potentials[9] of CuO/Cu_2O (0.669 V) and Cu_2O/Cu (0.471 V). This overpotential during cathodic reduction may be attributed to the potential barrier which emerges at the interface zone between Cu_2O (p type-semiconductor) and Cu substrate. The specimen anodically oxidized in the oxygen evolution region has two additional potential arrests of Φ_c^1 and $\Phi_c^{3'}$. Miller has suggested from his ring-disc copper electrode study[2] that the arrest potential of Φ_c^1 corresponds to the reduction of Cu_2O_3 to CuO. The potential arrest of $\Phi_c^{3'}$, however, has not been explained. It is considered that the potential barrier at the Cu_2O/Cu interface during cathodic reduction depends on the semiconductive property, i. e., nonstoichiometry of Cu_2O. The

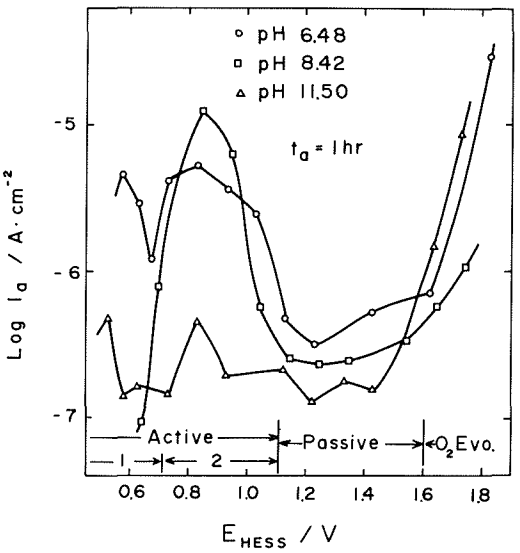

Fig. 1 Steady state-polarization curves of copper after 1 h-anodic oxidation in pH 6.48, 8.42 and 11.50 borate solutions.

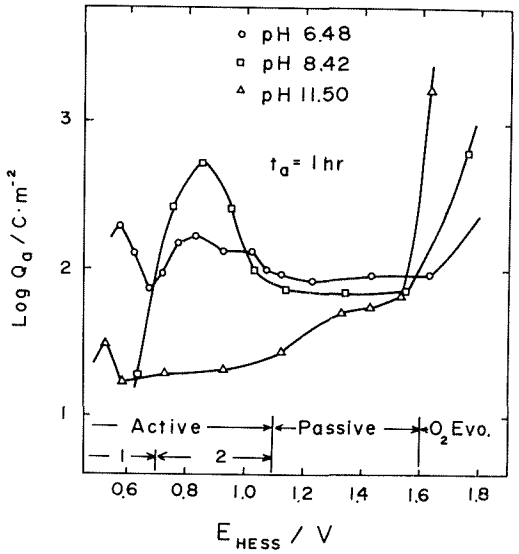

Fig. 2 Relation between electric charge Q_a passed during 1 h-anodic oxidation and anodic potential E_{HESS}.

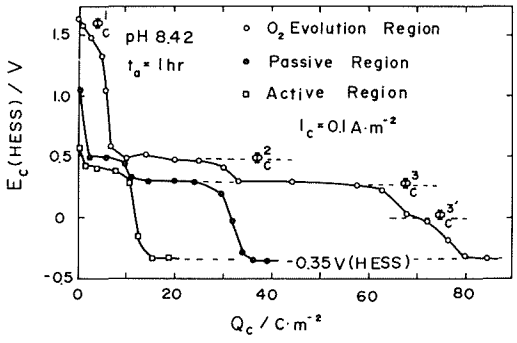

Fig. 3 Cathodic reduction curves of copper anodically oxidized for 1 h at potentials in the three different regions in PH 8.42 borate solution.

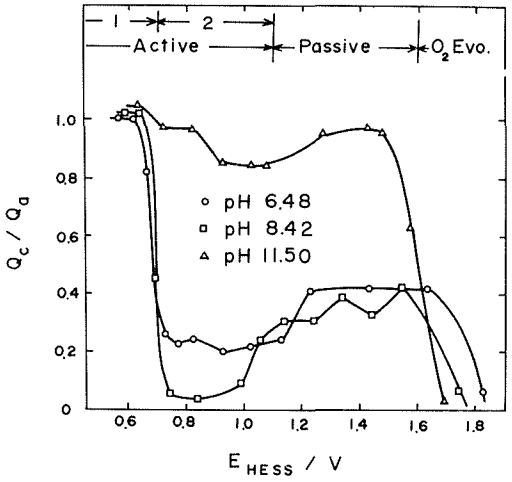

Fig. 4 Ratio of total cathodic charge Q_c required for film reduction to anodic charge Q_a passed during 1 h-anodic oxidation as a function of anodic potential E_{HESS}.

appearance of $\Phi_c^{3'}$ arrest, therefore, may be attributed to the change in non-stoichiometry of Cu_2O. The cathodic reduction is completed at −0.35 V (HESS), irrespective of the potential region of anodic oxidation. No dissolved cupric ions are detected during cathodic reduction, evidencing that the cathodic reduction proceeds through a solid state mechanism.[8]

As shown in Fig. 4, the total cathodic charge Q_c required for cathodic reduction is always less than the total anodic charge Q_a passed during anodic oxdation in all potential regions except the active potential region 1 in which Q_c is almost equal to Q_a. In Fig. 5, 6 and 7, the cathodic charges Q_c^1, Q_c^2 and Q_c^3, corresponding respectively to the durations of potential arrest at Φ_c^1, Φ_c^2 and Φ_c^3 are plotted as a function of anodic potential of film formation. The value of Q_c^3 in these figures involves that of $Q_c^{3'}$ corresponding to the duration of potential arrest at $\Phi_c^{3'}$

3. 3 Film thickness

The thickness of anodic oxide films formed on copper in the active and passive regions can be estimated from the values of Q_c^2 and Q_c^3 by using the following equations ;

$$L_{CuO} = \frac{Q_c^2 M_{CuO}}{F\rho_{CuO}}, \qquad (1)$$

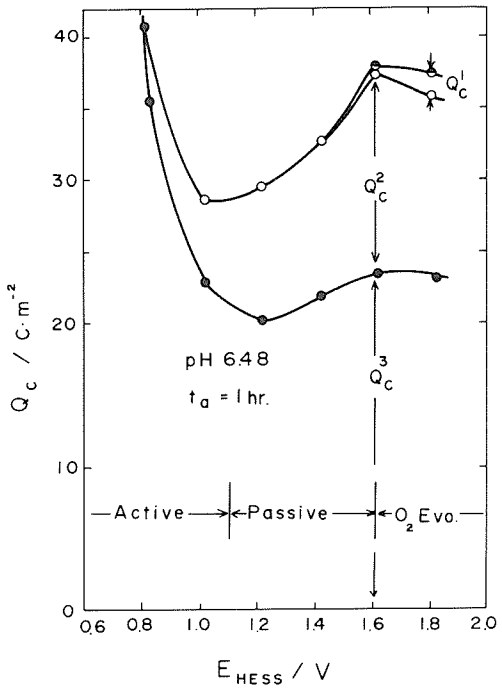

Fig. 5 Electric charge Q_c^1, Q_c^2 and Q_c^3 required for cathodic reduction of anodic oxide films formed on copper for 1 h in pH 6.48 borate solution as a function of anodic potential E_{HESS}. The values of Q_c^1, Q_c^2 and Q_c^3 correspond respectively to the duration of potential arrest at Φ_c^1, Φ_c^2 and Φ_c^3 in cathodic reduction curves. The value of Q_c^3 involves that of $Q_c^{3'}$ corresponding to the duration of potential arrest at $\Phi_c^{3'}$.

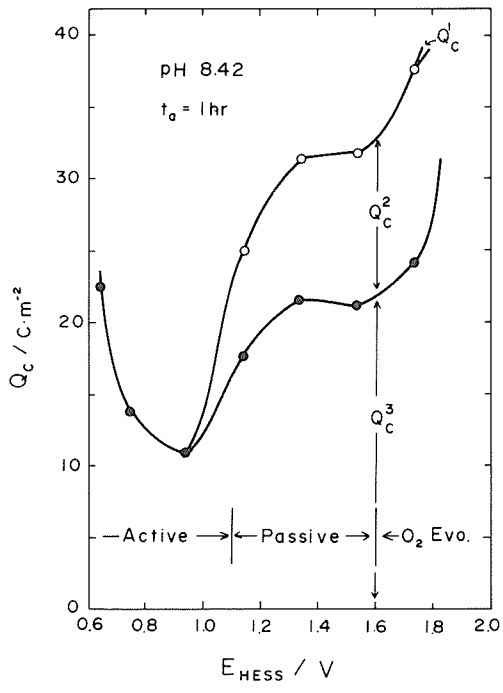

Fig. 6 Electric charge Q_c^1, Q_c^2 and Q_c^3 required for cathodic reduction of anodic oxide films formed on copper for 1 h in pH 8.42 borate solution as a function of anodic potential E_{HESS}. Designation of Q_c^1, Q_c^2 and Q_c^3 is the same as in Fig. 5.

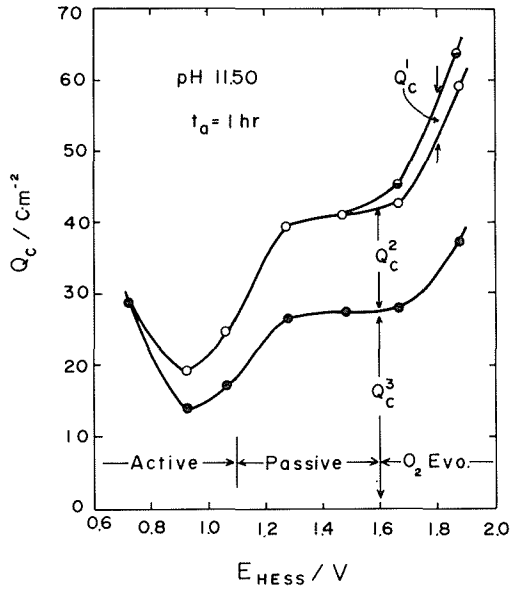

Fig. 7 Electric charge Q_c^1, Q_c^2 and Q_c^3 required for cathodic reduction of anodic oxide films formed on copper for 1 h in pH 11.50 borate solution as a function of anodic potential E_{HESS}. Designation of Q_c^1, Q_c^2 and Q_c^3 is the same as in Fig. 5.

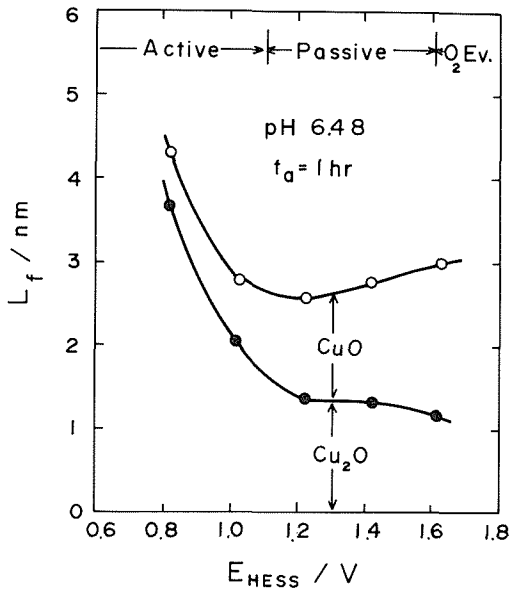

Fig. 8 Film thickness L_f coulometrically estimated for copper anodically oxidized for 1 h in pH 6.48 borate solution as a function of anodic potenial E_{HESS}.

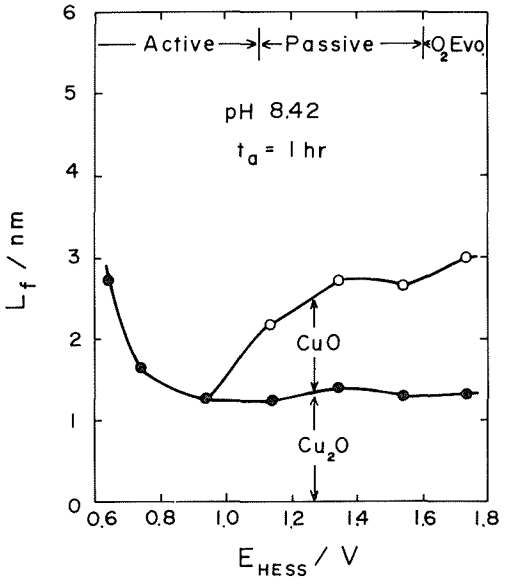

Fig. 9 Film thickness L_f, coulometrically estimated for copper anodically oxidized in pH 8.42 borate solution as a function of anodic potential E_{HESS}.

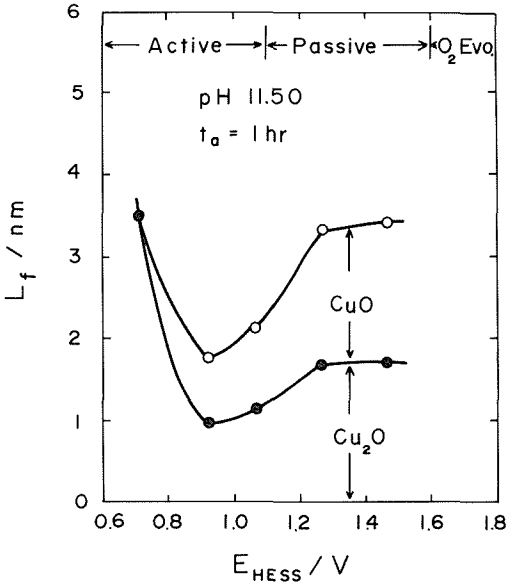

Fig. 10 Film thickness L_f, coulometrically estimated for copper anodically oxidized for 1 h in pH 11.50 borate solution as a function of anodic potential E_{HESS}.

$$L_{Cu_2O}=\frac{(Q_c^3-Q_c^2)M_{Cu_2O}}{F\rho_{Cu_2O}}, \quad (2)$$

where L_{CuO} is the thickness of the outer layer, L_{Cu_2O} the thickness of the inner layer, M_{CuO} the molecular weight of CuO, M_{Cu_2O} the molecular weight of Cu_2O, ρ_{CuO} the density of bulk CuO (6.45 g·cm^{-3}), ρ_{Cu_2O} the density of bulk Cu_2O (6.10 g · cm^{-3}), and F the Faraday constant. The film thickness, L_f, thus calculated is plotted versus anodic potential, E_{HESS} in Fig. 8, 9 and 10.

3. 4. AES and XPS analyses

Fig. 11 shows the Auger spectra of copper surface anodically oxidized for 1 h at 1.52 V (HESS) in pH 8.42 borate solution. The composition ratio, O/Cu, of anodic oxide films can be calculated by the following equation ;

$$O/Cu=\alpha\cdot H_O/H_{Cu}, \quad (3)$$

where α is the relative Auger sensitivity factor and H_O/H_{Cu} the Auger peak height ratio of Oxygen (510 eV) to Copper (920 eV). According to Hall and Morabito,[10] $\alpha=0.61$ was adopted for calculation of O/Cu. The depth-composition profiles of anodic oxide films formed on copper in pH 8.42 and 11.50 borate solutions are shown in Fig. 12 and 13. The sputtering time required for film removal is proportional to the total cathodic charge Q_C required for cathodic reduction. The presence of the plateau value of O/Cu nearly equal to Cu_2O in the observed depth-profiles proves that the inner layer of anodic oxide film is Cu_2O, whereas no O/Cu plateau corresponding to CuO is observed although the composition of uppermost surface approaches CuO as the potential increases. The Auger results, therefore, are not consistent with the electrochemical results which show the existence of CuO in the outer layer. This discrepancy may be caused by the alteration[11] of depth profiles due to argon ion sputter-etching. Particularly, the argon ion sputter-etching of the outer layer would give rise to the following reduction process ; $2CuO \rightarrow Cu_2O+\frac{1}{2}O_2$.

Fig. 14 shows the XPS spectra of Cu $2P_{3/2}$ and $2P_{1/2}$ of the specimen anodically oxidized in pH 8.42 borate solution. The Cu 2P spectra of the specimen anodically oxidized at the potential of 0.84V in the active region is in good agreement with that of metallic copper shown by

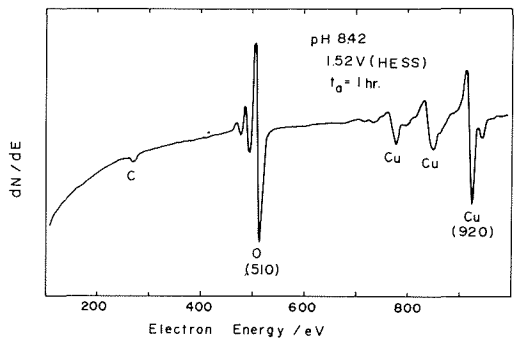

Fig. 11 Auger spectra of copper anodically oxidized for 1 h at 1.52 V (HESS) in pH 8.42 borate solution.

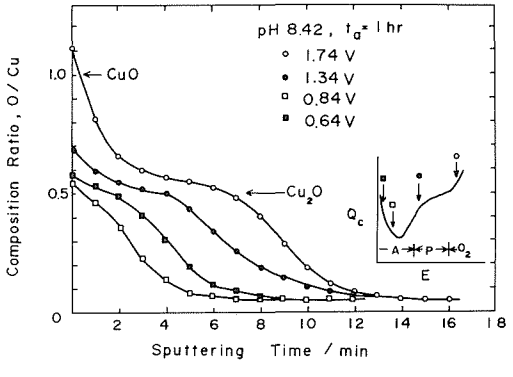

Fig. 12 Depth-composition profiles of copper anodically oxidized for 1 h at four different potentials in pH 8.42 borate solution. The marks of A, P and O_2 in figure represent the respective potential regions.

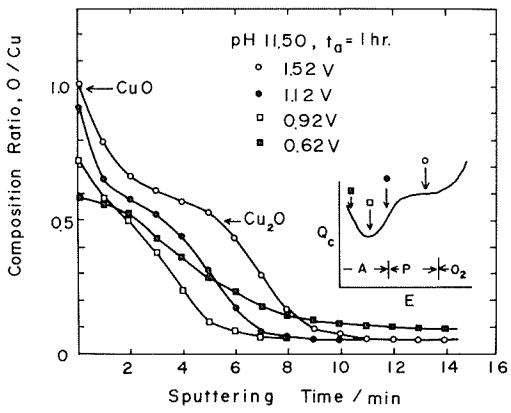

Fig. 13 Depth-composition profiles of copper anodically oxidized for 1 h at four different potentials in pH 11.50 borate solution. The marks of A, P and O_2 represent the respective potential regions.

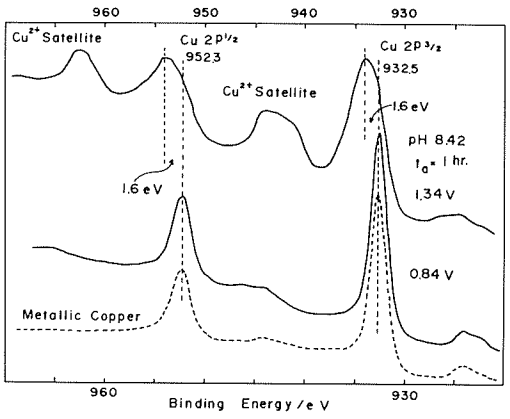

Fig. 14 XPS spectra of Cu 2P⅜ and 2P½ for copper anodically oxidized for 1 h at 0.84 V and 1.34 V in pH 8.42 borate solution. The dotted spectra in figure designates metallic copper.

dotted line in Fig. 14, in spite of the Auger results indicating the presence of Cu_2O. The difference of Cu 2P binding energy between zero- and mono-valent copper is so slight[12),13),14)] (less than 0.2 eV) that it is very difficult to distinguish cuprous oxide from metallic copper. The Cu 2P spectra of the specimen anodically oxidized at the potential of 1.34V (HESS) in the passive region, however, shifts to the high energy direction by 1.6eV in comparison with that of metallic copper and also possesses a satellite peak which evidences the presence of divalent copper. According to the literature,[13),14)] the Cu 2P⅔ spectra of divalent copper shifts to the high energy direction by 1.2 eV for CuO and by 1.8~2.3 eV for $Cu(OH)_2$ in comparison with that of metallic copper. The energy shift of 1.6 eV, therefore, suggests that the outer layer of the passive film consists partly of hydrated cupric oxide, i. e., $CuO_x(OH)_{2-2x}$. The XPS results similar to the spectra in Fig. 14 were also obtained for the specimens anodically oxidized in pH 6.48 and 11.50 borate solutions.

The O 1s spectra of Anodic oxide films shown in Fig. 15 provide further detailed information on the state of oxygen bound with divalent copper in the outer layer. The dotted lines vertically drawn in Fig. 15 designate the binding energy position corresponding to different states of oxygen previously reported.[15)] Robert et al.[15)] reported that lattice oxygen O^{2-} (530.4 eV) bound with mono-valent copper ions differed from the lattice oxygen O^{2-} (529.7 eV) bound with divalent copper ions. The change in shape of the broad O 1s spectra of anodic oxide films suggests that dehydration of the hydrated outer layer progresses with increasing anodic potential.

3. 5. Film formation mechanism

The value of Q_a/Q_c almost equal to unity observed in active region 1 indicates that cuprous oxide film is directly formed on copper without any dissolution of cuprous ions. In active region 2, however, the film formation of Cu_2O and the dissolution of cupric ions proceed simultaneously as evidenced from the value of Q_a/Q_c (<1) and from the results of solution analysis. In the passive region, the outer layer of cupric hydroxide $Cu(OH)_2$ is formed on the

inner layer by precipitation of dissolved cupric ions.

Passivation of copper is mainly caused by the formation of $Cu(OH)_2$ because of the high resistance of $Cu(OH)_2$ against ionic conduction. XPS analysis predicts that the following dehydration process of the outer later layer occurs predominantly at high anodic potentials in the passive region ;

$$OH^-_{oxide} \rightarrow H^+_{aq} + O^{2-}_{oxide} \qquad (4)$$

The dehydration process may be assisted by a high electric field that occurs in the outer layer during anodic polarization.

In contrast, it is considered that the cuprous oxide film does not contribute to the passivation of copper because Cu_2O is usually a p type-semiconductor in which positive holes participate in the anodic dissolution resulting in degradation of electrochemical stability of the film. In active region 2, the following reaction may occur ;

$$Cu^+_{oxide} + \oplus \rightarrow Cu^{2+}_{aq}, \qquad (5)$$

where cuprous ions in the oxide film may react with positive holes, $\oplus$, in the valence band accumulated on the uppermost surface to form dissolved cupric ions. A more quantitative discussion on the film formation mechanism, however, awaits further studies[16),17)] of semiconductive properties of copper anodic oxide films.

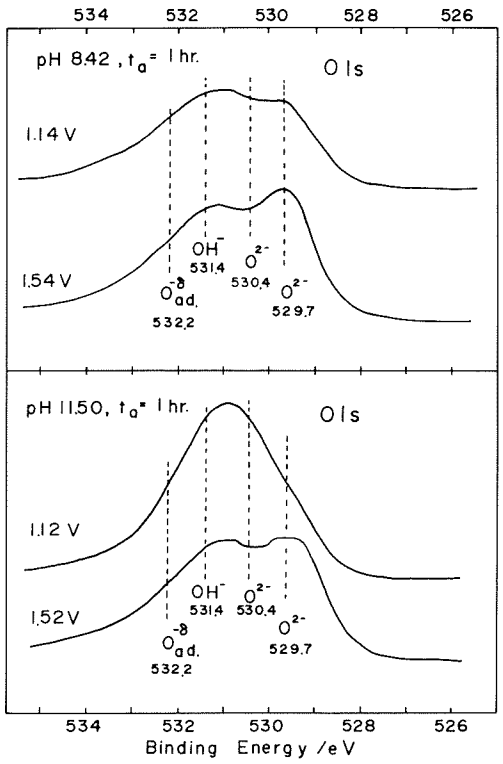

Fig. 15 XPS spectra of O 1s for copper anodically oxidized for 1 h at two different potentials in pH 8.42 and 11.50 borate solutions. The lines vertically drawn in figure designate the corresponding binding energy position of different O 1s states previously reported in literature.[15)]

4. Summary

Anodic oxide films formed potentionstatically on copper for 1 h in deaerated pH 6.48, 8.42 and 11.50 borate solutions were analyzed by using electrochemical techniques combined with Auger electron spectroscopy (AES) and X ray-photo electron spectroscopy (XPS). The anodic oxide films formed on copper in the passive region had a bi-layer structure which consisted of Cu_2O as an inner layer and a partly hydrated cupric oxide, $CuO_x(OH)_{2-2x}$ as an outer layer.

The active potential region of copper was divided into two parts ; anodic oxide films formed in active region 1 consisted of a single layer of Cu_2O, which was directly formed on the copper without any dissolution as cuprous ions into the solution, whereas in active region 2 the formation of Cu_2O and the dissolution of cupric ions proceeded simultaneously.

The dissolution-precipitation mechanism seemed likely to operate in the formation of $Cu(OH)_2$ as an outer layer leading to passivation of copper, whereas the dissolution mechanism

of Cu_2O in active region 2 was explained in terms of the p type- smiconductive property of Cu_2O.

Acknowledgement

The authors are indebted to Dr. H. Konno for conducting the XPS measurements.

Refernces

1) Shams, A. M., Din El & Abd El Wahab, F. M. : Electrochim. Acta, **9** (1964), p. 1131.
2) Miller, B. : J. Electrochem. Soc., **116** (1969), No. 12, p. 1675.
3) Dignam, M. J. & Gibbs, D. B. : Can. J. Chem., **48** (1970), p. 1242.
4) Ambrose, J., Barradas, R. G. & Shoesmith, D. W. : J. Electroanal. Chem., **47** (1973), p. 47, p. 65.
5) Shoesmith, D. W., Rummery, T. E., Owen, D. & Lee, W. : J. Electrochem. Soc., **123** (1976), No. 6, p. 790.
6) Ashworth, V. & Fairhurst, D. : J. Electrochem. Soc., **124** (1977), No. 4, p. 506.
7) Shoesmith, D. W., Rummery, T. E., Owen, D. & Lee, W. : Electrochim. Acta, **22**, (1977), No. 12, p. 1403.
8) Tsuru, T. & Haruyama, S. : J. Japan Inst. Met., **40** (1976), No. 11, p. 1172.
9) Pourbaix, M. : "Atlas of Electrochemical Equilibria in Aqueous Solutions", (1966), p. 384, Pergamon Press, London.
10) Hall, P. M. & Morabito, J. M. : Surface Sci., **67** (1977), No. 2, p. 373.
11) Kim, K. S. & Winograd, M. : Surface Sci., **43** (1974), p. 625.
12) Larson, P. E. ; J. Electron Spectrosc., **4** (1974), p. 213.
13) Barr, T. L. : J. Phys. Chem., **82** (1978), No. 16, p. 1801.
14) Mclntyre, N. S., Rummery, T. E., Cook, M. G. & Owen, D. : J. Electrochem. Soc., **123** (1986), No. 8, p. 1164.
15) Robert, T., Bartel, M. & Offergeld, G. : Surface Sci., **33** (1972), p. 123.
16) Paatsch, W. : Ber. Bunsenges. phys. Chem., **81** (1977), No. 7, p. 645.
17) Oshe, E. K. & Rosenfeld, I. L. : Boshoku Gijutsu, **29** (1980), No. 5, p. 215.